# Analytical and Experimental Considerations on the Resonant Frequency and the Quality Factor of Dielectric Resonators

MIKIO TSUJI, MEMBER, IEEE, HIROSHI SHIGESAWA, MEMBER, IEEE, HITOSHI AOKI, AND KEI TAKIYAMA, MEMBER, IEEE

*Abstract*—A dielectric pillbox resonator placed on a dielectric substrate is analyzed by a new method, the approximate mode matching method, in which the cross section of such a resonator is subdivided into several sub-sections having a simple geometry of the boundaries, i.e., dielectric slab radial waveguides, and the continuity condition of fields between subsections is treated in the least-squares sense.

The resonant frequencies and the intrinsic $Q$ values due to the leakage loss through the dielectric substrate calculated by this method are presented together with experimental results obtained in the 50-GHz region.

As a result, it is found that the experimental results for both the resonant frequencies and the $Q$ values agree better with our calculated ones than with the results by other approximate method, and so it will be concluded that the analytical method presented here is almost enough to discuss precisely the resonant characteristics of a dielectric pillbox resonator.

## I. Introduction

DIELECTRIC pillbox resonators have found practical applications, particularly in connection with the areas of both microwave and millimeter-wave circuits [1]–[7]. In such spectral regions, a dielectric pillbox is customarily installed in a metal waveguide or on a metallic ground plane, and their analyses have been performed by using several approximate methods, such as a magnetic wall model [7]–[10], a variational model [11], a dielectric waveguide model [12], and their mixed model [13], [14]. When this kind of resonator is employed in the short millimeter-wave region, a dielectric pillbox may be placed on a dielectric substrate to release a resonator from the inherent loss of metal. As expected easily from the existence of a dielectric substrate, the leakage of resonant energy occurs in the form of a surface wave which propagates away from the pillbox through the substrate. This situation will make it impossible to use most of the conventional approximate methods to calculate both the resonant frequency and the intrinsic $Q$ value due to the leakage loss.

So far as we know, the method reported by Marcatili [15] may be applicable to such a resonator after modifying the region made of only substrate into the homogeneous medium by means of the effective dielectric constant (EDC) method [16]. Marcatili's method is based on the approximate treatments of a dielectric rectangular waveguide neglecting the weakened fields in the so-called shaded area [17] and the $Q$ value due to the leakage loss is calculated in relation to its bending loss. Thus, for resonators less confining the fields in the dielectric pillbox, this method may give rise to large errors in calculation of the resonant characteristics. The purpose of this paper lies in the following two: one is to present a new approximate method which makes it easy to calculate precisely the $Q$ value as well as the resonant frequency for any dielectric pillbox resonator with a dielectric substrate, and the other is to demonstrate both the validity and the accuracy of our analysis by comparing with many results obtained by the careful and precise experiments in the 50-GHz region. Although the fields in the present analysis are approximated by neglecting the radiation fields with a continuous spectrum, the results obtained here prove that our analytical method gives reasonable and practical solutions for the resonant characteristics of dielectric pillbox resonators.

Manuscript received March 18, 1982; revised May 12, 1982.

The authors are with the Department of Electronics, Doshisha University, Kyoto, 602 Japan.

## II. Analysis

Fig. 1 shows the geometry of a dielectric pillbox resonator placed on a dielectric substrate. The radius of the pillbox is $R$ and its refractive index $n_1$ is related to the indices $n_2$, $n_3$, and $n_0$ of other regions by the condition that $n_1 \geq n_2 > n_3 \geq n_0$ (In this paper, the refractive index is used instead of the relative permittivity.) Although all dielectric materials involved here are considered to be isotropic and lossless, they are not the essential restriction for our analysis. As expected, the resonant modes in such a resonator are hybrid in the rigorous sense. Referring to [18], their fields can be expressed by using both TE and TM waves with respect to the $z$ direction and the resonant modes may be classified into the following two types. One type, which we call the HE mode hereafter, has the dominant contribution of the TE wave, while the other, the EH mode, has the dominant contribution of the TM wave. Although our attention in the following sections will be paid to the HE mode, the analytical procedure can be applied without distinction of the modal type.

The major difficulty in the analysis of this type of dielectric resonators lies in treating the irregular boundary of the structure which does not coincide with a separable geometry. Then let us subdivide the resonator into two constituent regions or building blocks, i.e., regions I and II, on the $\varphi - z$ cylindrical plane at $r = R$, and consider separately each of those regions as if they are slab radial waveguides [18] having four and three dielectric layers, respectively. We assume here that all the field components

0018-9480/82/1100-1952$00.75 ©1982 IEEE

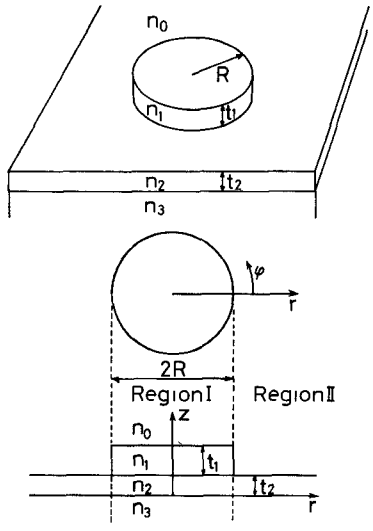


Fig. 1. Dielectric pillbox resonator on a dielectric substrate and the cylindrical coordinate system.

can be expanded in terms of the TE and TM propagating surface wave modes of the dielectric slab radial waveguide in each region, neglecting the radiation waves with a continuous spectrum. Then the fields of the resonator can be expressed by using the scalar potential functions, $\psi_i$ and $\bar{\psi}_i$ $(i = \mathrm{I}, \mathrm{II})$ as follows:

$$
\begin{aligned}
E_{ri} &= \frac{1}{j\omega\epsilon_0 n_j^2}\frac{\partial^2\bar{\psi}_i}{\partial r\,\partial z} - \frac{1}{r}\frac{\partial\psi_i}{\partial\varphi} \\
E_{\varphi i} &= \frac{1}{j\omega\epsilon_0 n_j^2 r}\frac{\partial^2\bar{\psi}_i}{\partial\varphi\,\partial z} + \frac{\partial\psi_i}{\partial r} \\
E_{zi} &= \frac{1}{j\omega\epsilon_0 n_j^2}\left(\frac{\partial^2}{\partial z^2} + n_j^2 k_0^2\right)\bar{\psi}_i \\
H_{ri} &= \frac{1}{r}\frac{\partial\bar{\psi}_i}{\partial\varphi} + \frac{1}{j\omega\mu_0}\frac{\partial^2\psi_i}{\partial r\,\partial z} \\
H_{\varphi i} &= -\frac{\partial\bar{\psi}_i}{\partial r} + \frac{1}{j\omega\mu_0 r}\frac{\partial^2\psi_i}{\partial\varphi\,\partial z} \\
H_{zi} &= \frac{1}{j\omega\mu_0}\left(\frac{\partial^2}{\partial z^2} + n_j^2 k_0^2\right)\psi_i
\end{aligned}
\tag{1}
$$

where

$$
\begin{aligned}
\psi_i &= \cos\nu\varphi\sum_m A_{mi}F_\nu(\rho_{mi}r)g_{mi}(z)e^{j\omega t} \\
\bar{\psi}_i &= \sin\nu\varphi\sum_m \bar{A}_{mi}F_\nu(\bar{\rho}_{mi}r)\bar{g}_{mi}(z)e^{j\omega t} \qquad (i = \mathrm{I}, \mathrm{II}).
\end{aligned}
\tag{2}
$$

In these expressions, the upper bar is put on all quantities related to the TM wave and $k_0$ is the wave number in the free space. $A_{mi}$ and $\bar{A}_{mi}$ are modal expansion coefficients to be determined, and the function of the radial coordinate $F_\nu$ is given by

$$
F_\nu(u) = \begin{cases} J_\nu(u), & \text{for region I} \\ H_\nu^{(2)}(u), & \text{for region II,} \end{cases}
\tag{3}
$$

where $J_\nu$ and $H_\nu^{(2)}$ are the first kind of the Bessel function and the second kind of the Hankel function of the $\nu$th order, respectively, and $\nu$ must be an integer. The $\rho_{mi}$ and $\bar{\rho}_{mi}$ are wavenumbers in the radial direction and $g_{mi}(z)$ and $\bar{g}_{mi}(z)$ the modal functions of the $m$th TE and TM modes in the slab radial waveguide. For example, $g_{m\mathrm{I}}(z)$ and $g_{m\mathrm{II}}(z)$ are given as

$$
g_{m\mathrm{I}}(z) = \begin{cases} \sin(\beta_{m\mathrm{I}}t_1 + \theta_{m\mathrm{I}})e^{-\alpha_{m\mathrm{I}}\{z-(t_1+t_2)\}}, & t_1 + t_2 \leqslant z \\ \sin\{\beta_{m\mathrm{I}}(z - t_2) + \theta_{m\mathrm{I}}\}, & t_2 \leqslant z \leqslant t_1 + t_2 \\ \dfrac{\sin\theta_{m\mathrm{I}}}{\sinh(\delta_{m\mathrm{I}}t_2 + \xi_{m\mathrm{I}})}\sinh(\delta_{m\mathrm{I}}z + \xi_{m\mathrm{I}}), & 0 \leqslant z \leqslant t_2 \\ \dfrac{\sin\theta_{m\mathrm{I}}\sinh\xi_{m\mathrm{I}}}{\sinh(\delta_{m\mathrm{I}}t_2 + \xi_{m\mathrm{I}})}e^{\gamma_{m\mathrm{I}}z}, & z \leqslant 0 \end{cases}
\tag{4}
$$

$$
g_{m\mathrm{II}}(z) = \begin{cases} \sin(\kappa_{m\mathrm{II}}t_2 + \theta_{m\mathrm{II}})e^{-\alpha_{m\mathrm{II}}(z-t_2)}, & t_2 \leqslant z \\ \sin(\kappa_{m\mathrm{II}}z + \theta_{m\mathrm{II}}), & 0 \leqslant z \leqslant t_2 \\ \sin\theta_{m\mathrm{II}}e^{\gamma_{m\mathrm{II}}z}, & z \leqslant 0 \end{cases}
\tag{5}
$$

with the conservation relations of wavenumbers:

$$
\begin{aligned}
\left(n_1\frac{\omega}{c}\right)^2 &= \rho_{m\mathrm{I}}^2 + \beta_{m\mathrm{I}}^2 \\
\left(n_2\frac{\omega}{c}\right)^2 &= \rho_{m\mathrm{I}}^2 - \delta_{m\mathrm{I}}^2 = \rho_{m\mathrm{II}}^2 + \kappa_{m\mathrm{II}}^2 \\
\left(n_3\frac{\omega}{c}\right)^2 &= \rho_{m\mathrm{I}}^2 - \gamma_{m\mathrm{I}}^2 = \rho_{m\mathrm{II}}^2 - \gamma_{m\mathrm{II}}^2 \\
\left(n_0\frac{\omega}{c}\right)^2 &= \rho_{m\mathrm{I}}^2 - \alpha_{m\mathrm{I}}^2 = \rho_{m\mathrm{II}}^2 - \alpha_{m\mathrm{II}}^2
\end{aligned}
\tag{6}
$$

where $c$ is the velocity of light in the free space. The $\theta_{m\mathrm{I}}$, $\xi_{m\mathrm{I}}$, and $\theta_{m\mathrm{II}}$ are constants that locate the field maxima in regions I and II.

The $\bar{g}_{m\mathrm{I}}(z)$ and $\bar{g}_{m\mathrm{II}}(z)$ for the TM mode can be given by the same expressions as those in (4), (5), and (6) if putting the upper bar on the quantities related to the TM mode, and so they are omitted in this paper. Here, the boundary conditions on the $r$–$\varphi$ plane at $z = 0$, $t_1$ and $t_2$ define the wavenumbers in the $z$ direction through the following eigenvalue equations:

$$
\begin{aligned}
\tan\beta_{m\mathrm{I}}t_1 &= \frac{\beta_{m\mathrm{I}}\{\delta_{m\mathrm{I}}(\alpha_{m\mathrm{I}} + \gamma_{m\mathrm{I}}) + (\delta_{m\mathrm{I}}^2 + \alpha_{m\mathrm{I}}\gamma_{m\mathrm{I}})\tanh\delta_{m\mathrm{I}}t_2\}}{\delta_{m\mathrm{I}}(\beta_{m\mathrm{I}}^2 - \gamma_{m\mathrm{I}}\alpha_{m\mathrm{I}}) + (\beta_{m\mathrm{I}}^2\gamma_{m\mathrm{I}} - \delta_{m\mathrm{I}}^2\alpha_{m\mathrm{I}})\tanh\delta_{m\mathrm{I}}t_2} \\
\tan\kappa_{m\mathrm{II}}t_2 &= \frac{\kappa_{m\mathrm{II}}(\alpha_{m\mathrm{II}} + \gamma_{m\mathrm{II}})}{\kappa_{m\mathrm{II}}^2 - \gamma_{m\mathrm{II}}\alpha_{m\mathrm{II}}}
\end{aligned}
\tag{7}
$$

for TE waves and

$$
\begin{aligned}
\tan\bar{\beta}_{m\mathrm{I}}t_1 &= \frac{\eta_1^2\bar{\beta}_{m\mathrm{I}}\{\bar{\delta}_{m\mathrm{I}}(\eta_3^2\bar{\alpha}_{m\mathrm{I}} + \eta_0^2\bar{\gamma}_{m\mathrm{I}}) + (\eta_0^2\eta_3^2\bar{\delta}_{m\mathrm{I}}^2 + \bar{\alpha}_{m\mathrm{I}}\bar{\gamma}_{m\mathrm{I}})\tanh\bar{\delta}_{m\mathrm{I}}t_2\}}{\bar{\delta}_{m\mathrm{I}}(\eta_0^2\eta_3^2\bar{\beta}_{m\mathrm{I}} - \eta_1^2\bar{\gamma}_{m\mathrm{I}}\bar{\alpha}_{m\mathrm{I}}) + (\eta_0^2\bar{\beta}_{m\mathrm{I}}^2\bar{\gamma}_{m\mathrm{I}} - \eta_1^4\eta_3^2\bar{\delta}_{m\mathrm{I}}^2\bar{\alpha}_{m\mathrm{I}})\tanh\bar{\delta}_{m\mathrm{I}}t_2} \\
\tan\bar{\kappa}_{m\mathrm{II}}t_2 &= \frac{\bar{\kappa}_{m\mathrm{II}}(\eta_3^2\bar{\alpha}_{m\mathrm{II}} + \eta_0^2\bar{\gamma}_{m\mathrm{II}})}{\eta_3^2\eta_0^2\bar{\kappa}_{m\mathrm{II}}^2 - \bar{\alpha}_{m\mathrm{II}}\bar{\gamma}_{m\mathrm{II}}}
\end{aligned}
\tag{8}
$$

for TM waves, where

$$\eta_0 = n_0/n_2, \quad \eta_1 = n_1/n_2, \quad \eta_3 = n_3/n_2. \tag{9}$$

It is obvious that the characteristic angular resonant frequency $\Omega$ is determined by the remaining boundary condition on the $z-\varphi$ cylindrical plane at $r = R$. In other words, the simultaneous continuity conditions $\mathbf{r}\times(\mathbb{E}_{\mathrm{I}} - \mathbb{E}_{\mathrm{II}}) = 0$ and $\mathbf{r}\times(\mathbb{H}_{\mathrm{I}} - \mathbb{H}_{\mathrm{II}}) = 0$ have to be solved, where $\mathbf{r}$ is the unit vector to the radial direction. However, this type of boundary conditions is never satisfied by the approximating fields employed here, so let us fit the fields to these boundary conditions in the sense of least-squares [19]. For this purpose, the mean-squares error E is introduced in the boundary condition defined by the following equation:

$$\mathrm{E} = \int_0^{2\pi}\int_{-\infty}^{\infty} \{|\mathbf{r}\times(\mathbb{E}_{\mathrm{I}} - \mathbb{E}_{\mathrm{II}})|^2_{r=R} + Z_{ni}^2|\mathbf{r}(\mathbb{H}_{\mathrm{I}} - \mathbb{H}_{\mathrm{II}})|^2_{r=R}\} R\, dz\, d\varphi \tag{10}$$

where $Z_{ni} = \mu_0/n_i^2\epsilon_0$ is the intrinsic impedance of medium $n_i$. After substituting (1)–(6) into (10) and performing the integrations, the error E can be expressed as follows:

$$\mathrm{E} = \sum_{i=\mathrm{I},\,\mathrm{II}} \sum_{i'=\mathrm{I},\,\mathrm{II}} \sum_m \sum_{m'} \{A_{mi}A^*_{m'i'}P_{mm'ii'}(\omega) + A_{mi}\bar{A}^*_{m'i'}Q_{mm'ii'}(\omega) + A^*_{mi}\bar{A}_{m'i'}Q^*_{mm'ii'}(\omega) + \bar{A}_{mi}\bar{A}^*_{m'i'}R_{mm'ii'}(\omega)\} \tag{11}$$

where the symbol * denotes the complex conjugate and $P$, $Q$, and $R$ are the functions of only the angular frequency $\omega$, of which explicit but tedious forms can be found in [20]. The characteristic angular resonant frequency $\Omega$ will then be obtained by means of the Ritz–Galerkin variational approach to this E. So, we minimize E with respect to the unknown variables, that is, the modal expansion coefficients and the angular frequency $\omega$, and obtain the $\Omega$ by the same procedure described in [21].

As a result, the characteristic angular resonant frequency for a mode is found as the complex quantity

$$\Omega = \omega_r + j\omega_i \tag{12}$$

where both $\omega_r$ and $\omega_i$ must be positive for the so-called damped free oscillation because of the leakage field expressed by the second kind of the Hankel function. Therefore, the resonant frequency $f_0$ and the intrinsic $Q$ value $Q_0$ can be calculated from $\Omega$ as follows:

$$f_0 = |\Omega|/2\pi, \quad Q_0 = |\Omega|/2\omega_i. \tag{13}$$

## III. Numerical Results

In the spectral range from the short millimeter to the submillimeter waves, most of the solid dielectric materials show a considerable absorption loss and only a few nonpolar polymers, e.g., polyethylene, show somewhat low absorptions. However, all of these polymers have almost the same low refractive indices (around 1.5), so that it will be necessary to construct a resonator by using the same dielectric material for both pillbox and substrate. In such a case, the field confinement in the pillbox becomes weak in general, and for obtaining the high $Q$ value, it is necessary that such a resonator functions with a edge-guided resonant mode which can exist in the pillbox with a relatively large radius $R$ compared to the wavelength, that is, in a higher order mode in the $\varphi$ direction having a large $\nu$. Thus, in numerical calculations, the pillbox resonator is considered which consists of the polyethylene ($n_1 = n_2 = 1.51$)[1] and the air ($n_0 = n_3 = 1.0$) with a large $R$.

In the following section, the scaled experiments in the 50-GHz region will be performed in order to confirm the accuracy of our analytical approach, so the numerical results are also compared in this frequency region, where the thickness of the pillbox and the substrate are assumed to be $t_1 = 2.0$ mm and $t_2 = 1.0$ mm, respectively. For this structure, the slab radial waveguide with thickness $t_2$ (region II) can support only the fundamental TE and TM modes indicated with $m = 1$ in (5), so that resonant modes will be designated as $\mathrm{HE}_{pq\nu}$ ($\mathrm{EH}_{pq\nu}$) where the subindices $p$ and $q$ represent the number of extrema of the $E_{r\mathrm{I}}$ ($H_{r\mathrm{I}}$) component in the $z$ and $r$ directions in the region I, respectively.

The typical results of the resonant frequency $f_0$ and the intrinsic $Q$ value $Q_0$ due to the leakage loss are shown in Table I for the $\mathrm{HE}_{11}$ mode ($\nu = 50$) and also the $\mathrm{TE}_{11}$-like mode ($\nu = 50$) which is a rough approximation for the $\mathrm{HE}_{11}$ mode neglecting the contribution of the TM wave in (1). Also, this table compares with the results by Marcatili's approximate method supported by the EDC method, where the resonant mode will be designated as $\mathrm{H}_{11}^z$ mode. We can find that in case of $R = 40$ mm, the resonant frequency of the $\mathrm{TE}_{11}$-like mode is higher than that of the $\mathrm{HE}_{11}$ mode by about $+0.18$ percent (90 MHz), while Marcatili's one is much higher by about $+0.42$ percent (200 MHz). Such a tendency is obviously seen in all values of $R$. Moreover, we will observe in the following section that the measured results show a fairly good agreement with our results of the $\mathrm{HE}_{11}$ mode. Considering that the difference in the resonant frequency mentioned above is significant when devising, for instance, a frequency diplexer, one should be careful in using Marcatili's method even for estimating the resonant frequency.

On the other hand, the difference between our results ($\mathrm{HE}_{11}$) and Marcatili's ones ($\mathrm{H}_{11}^z$) for the intrinsic $Q$ value is more remarkable than that for the resonant frequency. Again, the later experiments will show a significant disagreement with the results of Marcatili's approach. The large error included in his method may be mainly caused by the following two rough approximations. One of them is the assumption of the existence of the so-called shaded area [17] in case of good confinement of the fields in a pillbox and the other is the introduction of Watson's approximation [22] to $J_\nu(u)$ and $H_\nu^{(2)}(u)$ assuming $\nu^2/(u_r^2 - \nu^2) \ll 1$, where $u_r$ is the real part of $u$. In the resonator considered here, the confinement of the fields is loose in both the $z$ and the $r$ directions and also $\nu^2/(u_r^2 - \nu^2)$ is about $0.2 \sim 0.3$. Therefore, it may be concluded that Marcatili's approach no longer gives any reliable results for the resonators having the structure discussed here. In contrast to this, our method based on the mode-matching procedure is free from the above-mentioned approximations which may be effective only in the optical region, and

[1] Measured value for the polyethylene used in our experiments.

TABLE I
COMPARISON OF RESONANT FREQUENCIES AND INTRINSIC $Q$ VALUES CALCULATED BY THE VARIOUS APPROXIMATE METHODS

| Radius R (mm) | $HE_{11}$ mode | | $TE_{11}$ like mode | | Marcatili's Method | |
|---|---|---|---|---|---|---|
| | Resonant Frequency (GHz) | Intrinsic Q $Q_0$ | Resonant Frequency (GHz) | Intrinsic Q $Q_0$ | Resonant Frequency (GHz) | Intrinsic Q $Q_0$ |
| 35 | 53 95 | 179 | 54 05 | 179 | 54.21 | 136 |
| 40 | 47 94 | 241 | 48 03 | 238 | 48 14 | 167 |
| 45 | 43 19 | 296 | 43 24 | 292 | 43 40 | 184 |
| 50 | 39 41 | 308 | 39 45 | 302 | 39 59 | 187 |
| 55 | 36 30 | 297 | 36 33 | 293 | 36 45 | 179 |
| 60 | 33 68 | 273 | 33 70 | 271 | 33 82 | 163 |
| 65 | 31 45 | 246 | 31 46 | 243 | 31 57 | 145 |

may precisely calculate the resonant characteristics for any structure of a resonator in the short millimeter-wave region. This will be successfully confirmed through the experiments in the following section.

Finally, the calculated results shown in Table I are summarized in Fig. 2(a) and (b), which also exhibits the results of $HE_{11\nu}$ with $\nu = 75$. In this figure, the intrinsic $Q$ value has the maximum value at a definite value of $R$. The degree of field concentration in the pillbox will explain physically this interesting phenomenon. Approximating the $HE_{11}$ mode by the $TE_{11}$-like mode, one can calculate the effective indices of refraction $n_{\mathrm{eff\,I}}$ for the region I and $n_{\mathrm{eff\,II}}$ for the region II from the ratio $\rho_{1\mathrm{I}}/k_0$ and $\rho_{1\mathrm{II}}/k_0$, respectively. It is easily shown that the larger the ratio $n_{\mathrm{eff\,I}}/n_{\mathrm{eff\,II}}$ becomes, the more the field is confined in the pillbox, and the $Q_0$ value will increase monotonically. However, the present case considers the $HE_{11}$ mode with fixed $\nu$ ($= 50$), and its resonant frequency varies as a function of $R$ as shown in Fig. 2(a), so that the ratio $n_{\mathrm{eff\,I}}/n_{\mathrm{eff\,II}}$ also varies with $R$ as shown in Fig. 3. The $Q_0$ value will then vary according to this curve, which explains well the result of Fig. 2(b).

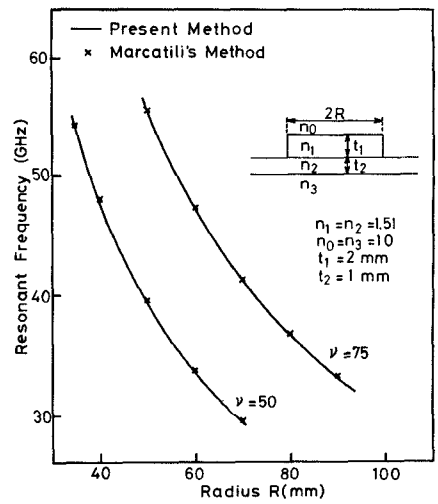


(a)

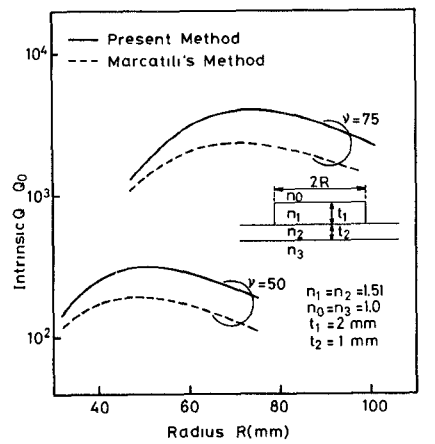


(b)

Fig. 2. Comparison of the numerical results between the present method and Marcatili's one. (a) Resonant frequency. (b) Intrinsic $Q$ value.

## IV. EXPERIMENTS

### A. Experimental Setup

The experimental setup in the 50 GHz is shown schematically in Fig. 4, where the construction of the pillbox resonator tested is the same as that described in Section III. In this setup, the polyethylene plate of a one-by-one meter in size is used as a substrate and its outer edges are terminated with an absorber (Eccosorb) so that the measurements do not suffer the influence of the reflection of the leaky wave propagating through the substrate toward the outside of a pillbox. The millimeter-wave power from the klystron is launched into a polyethylene rib waveguide having the dimensions shown in the inset of Fig. 4. The pillbox is coupled with this waveguide through a suitable coupling gap $D$. In this arrangement, the coupling occurs unidirectionally if the output end of the rib waveguide is terminated with a matched load, and brings on the resonance of traveling wave type. Thus, the resonant characteristics can be obtained by measuring the ratio of the output power of the rib waveguide with a pillbox to that without it. On the other hand, if the rib waveguide is terminated with a short circuit, the coupling with the pillbox occurs bidirectionally, and causes a standing-wave type resonance of which the standing-wave pattern along the circumference of the pillbox can be utilized to identify the resonant order $\nu$ of a mode.

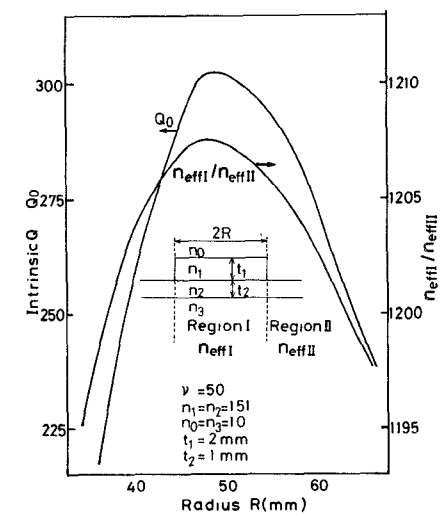


Fig. 3. Variation of the ratio $n_{\mathrm{eff\,I}}/n_{\mathrm{eff\,II}}$ of the effective indices of refraction and the intrinsic $Q$ value for various radii of the pillbox.

### B. Experimental Results

Launching a wave polarized parallel to the $x$ axis (see Fig. 4), the rib waveguide propagates the TE-like mode

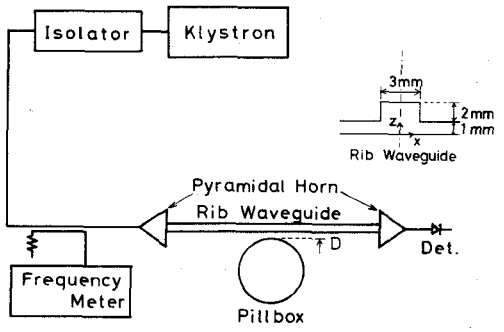


Fig. 4. Schematic diagram of the experimental setup.

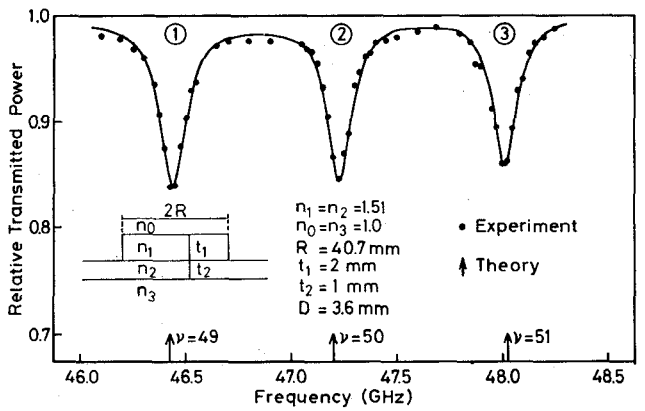


Fig. 5. Resonant characteristics obtained from the relative transmitted power of the rib waveguide.

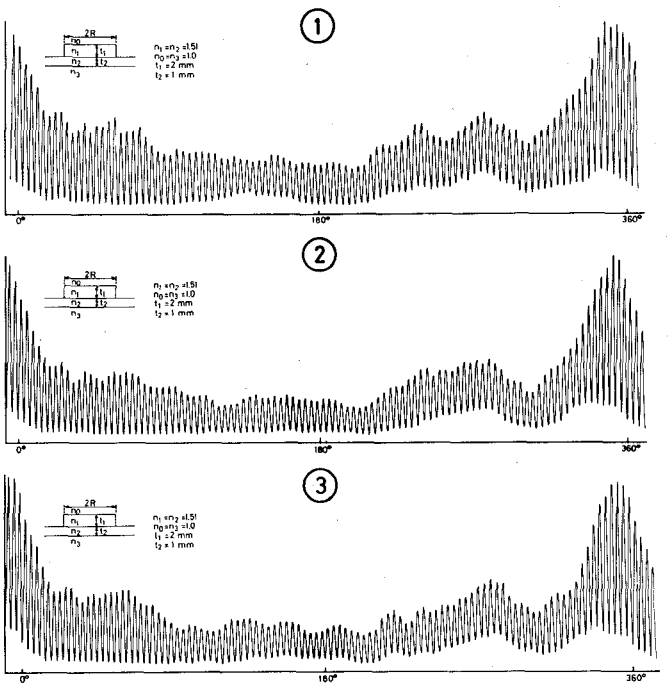


Fig. 6. Standing-wave patterns at the resonant points ①, ②, and ③ in Fig. 4 measured along the circumference of the pillbox.

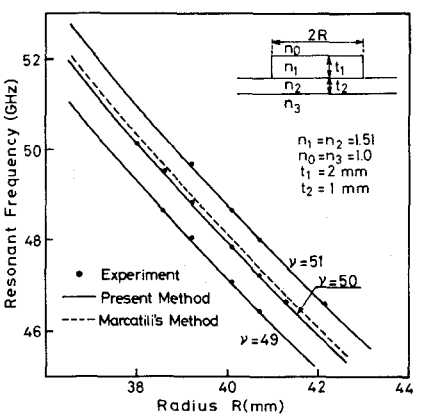


Fig. 7. Measured resonant frequencies of the $HE_{11\nu}$ mode for various radii of the pillbox ($\nu = 49$, 50, and 51).

which is indeed the hybrid mode, but is polarized predominantly in the $x$ direction, so that the resonance of HE modes can be expected in the pillbox. Fig. 5 shows the typical resonant characteristics for such a case, where $R = 40.7$ mm and $D = 3.6$ mm are chosen. It is clearly shown in this figure that there are three resonant points indicated by ①, ②, and ③ corresponding to the measured resonant frequencies of $f_0 = 46.44$, 47.23, and 48.01 GHz, respectively. To confirm the resonant order $\nu$ at each resonant point, the standing-wave patterns are then measured by means of the electric field probe [23]. The results are shown in Fig. 6, and it may be concluded from this figure that the resonant orders at the resonant points ①, ②, and ③ are $\nu = 49$, 50, and 51, respectively.

On the other hand, the theoretical resonant frequencies of the $HE_{11}$ mode with $\nu = 49$, 50, and 51 are calculated as $f_0 = 46.43$, 47.21, and 48.03 GHz, respectively. These frequencies, indicated by the mark (↑) on the abscissa of Fig. 5, are in fairly good agreement with the observed frequencies at the resonant points ①, ②, and ③, respectively. Moreover, the next higher order mode is the $HE_{12}$ mode, and its resonant frequency is found to be, for instance, 51.3 GHz for $\nu = 50$ which is far from the observed frequency at the resonant point ② by about 4 GHz. From these discussions, we may conclude that the resonant modes observed at the points ①, ②, and ③ are the $HE_{11}$ mode with $\nu = 49$, 50, and 51, respectively.

Fig. 7 summarizes the measured resonant frequencies of the $HE_{11}$ mode for other $R$-values. The solid lines indicate the theoretical values calculated by the present method, while the dashed line indicates those by Marcatili's method for $\nu = 50$. As seen from this figure, our results show a satisfactory agreement with experimental ones, but the dashed line is different from them by about 200 MHz in the 50-GHz region.

On the other hand, Fig. 8 shows the comparison between the measured and theoretical intrinsic $Q$ values for $\nu = 49$, 50, and 51. The solid lines show our theoretical values, while the dashed lines show the results by Marcatili's method. In our experiments, the intrinsic $Q$ value is obtained from the best-fitted Lorentzian for the measured resonant curve by assuming that the coupling between the pillbox and the rib waveguide is small enough and the adjacent resonances interfere little with each other as observed in Fig. 5. Note here that the $\tan\delta$ of a polyethylene is of the order of $10^{-4}$ in the 50-GHz region, so that we may accept that the measured $Q$ values are mainly due to the leakage loss through the dielectric substrate. It is obvious that the measured $Q_0$ values have the tendency to agree well with our results, but they do not change clearly among the adjacent resonant modes, so that it is hard to under-

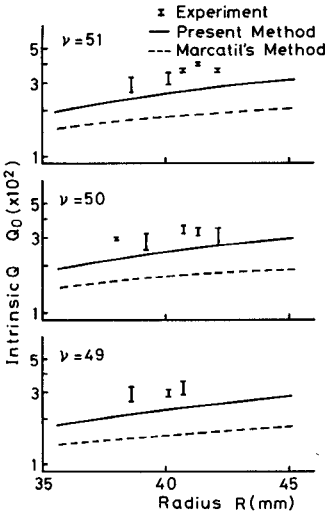


Fig. 8. Measured intrinsic $Q$ values of the $HE_{11\nu}$ mode for various radii of the pillbox ($\nu = 49$, 50, and 51).

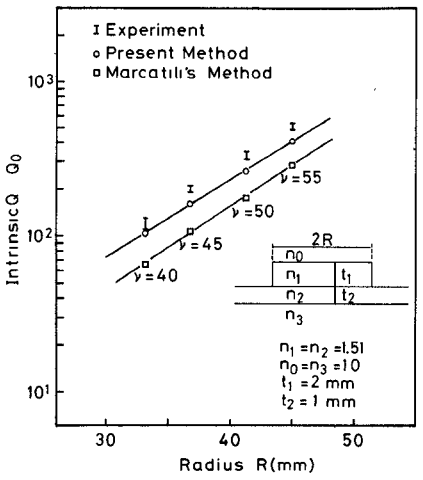


Fig. 9. Measured intrinsic $Q$ values of the $HE_{11\nu}$ mode for various radii of the pillbox ($\nu = 40$, 45, 50, and 55).

stand a definite variation of $Q_0$ to $\nu$. The $Q_0$ values measured for the $HE_{11}$ mode with other resonant orders $\nu$ are shown in Fig. 9. All of these pillboxes are designed so as to have the same resonant frequency $f_0 = 46.8$ GHz and also the theoretical values obtained at discrete points are linked one another by the curves for convenience sake. It is confirmed clearly from Figs. 8 and 9 that the measured intrinsic $Q$ values agree better with our theoretical ones than with Marcatili's ones, but are slightly higher than ours. This difference may be caused mainly by a poor approximation for the fields of a resonator. Nevertheless, the experimental measurements in this section will conclude that the analytical method presented here is almost enough in practice to calculate the intrinsic $Q$ value as well as the resonant frequency of the pillbox resonator with the dielectric substrate.

## V. Conclusion

The analytical method for dielectric pillbox resonators described here is based on the mode-matching technique in which the approximate fields satisfy the boundary conditions in the least-square sense. Although the fields are roughly approximated in the present analysis, the approach can be applied to any kind of dielectric pillbox resonators without unpermissible approximations which sometimes appear in the published methods. The calculated results sufficiently explain the experimental results of both the resonant frequency and the intrinsic $Q$ value due to the leakage loss through the dielectric substrate. The present analysis is a straightforward and effective method for investigating the resonant characteristics of a dielectric pillbox resonator.

## References

[1] D. J. Masse and R. A. Pucel, "A temperature stable bandpass filter using dielectric resonators," *Proc. IEEE*, vol. 60, pp. 730–731, June 1972.

[2] E. Fox, "Temperature stable low-loss microwave filters using dielectric resonators," *Electron. Lett.*, vol. 8, pp. 582–583, Nov. 1972.

[3] W. Harrison, "A miniature high $Q$ bandpass filter employing dielectric resonators," *IEEE Trans. Microwave Theory Tech.*, vol. MTT-16, pp. 218–227, Apr. 1968.

[4] T. D. Iveland, "Dielectric resonators filters for applications in microwave integrated circuits," *IEEE Trans. Microwave Theory Tech.*, vol. MTT-19, pp. 643–652, July 1971.

[5] M. A. Gerdine, "A frequency stabilized microwave band-rejection filter using high dielectric constant resonators," *IEEE Trans. Microwave Theory Tech.*, vol. MTT-17, pp. 354–359, July 1969.

[6] A. Karp, H. J. Shaw, and D. K. Winslow, "Circuits properties of microwave dielectric resonators," *IEEE Trans. Microwave Theory Tech.*, vol. MTT-16, pp. 818–828, Oct. 1968.

[7] S. B. Cohn, "Microwave bandpass filters containing high $Q$ dielectric resonators," *IEEE Trans. Microwave Theory Tech.*, vol. MTT-16, pp. 210–217, Apr. 1968.

[8] H. M. Schlicke, "Quasi-degenerated modes in high $\epsilon$ dielectric cavities," *J. Appl. Phys.*, vol. 24, pp. 187–191, Feb. 1953.

[9] H. Y. Yee, "Natural resonant frequencies of microwave dielectric resonators," *IEEE Trans. Microwave Theory Tech.*, vol. MTT-13, p. 256, Mar. 1965.

[10] A. Okaya and L. F. Barash, "The dielectric microwave resonators," *Proc. IRE*, vol. 50, pp. 2081–2092, Oct. 1962.

[11] Y. Konishi, N. Hoshino, and Y. Utsumi, "Resonant frequency of a $TE_{01\delta}$ dielectric resonator," *IEEE Trans. Microwave Theory Tech.*, vol. MTT-24, pp. 112–114, Feb. 1976.

[12] T. Itoh and R. Rudokas, "New method for computing the resonant frequencies of dielectric resonators," *IEEE Trans. Microwave Theory Tech.*, vol. MTT-25, pp. 52–54, Jan. 1977.

[13] Y. Garault and P. Guillon, "Higher accuracy for the resonance frequencies of dielectric resonators," *Electron. Lett.*, vol. 12, pp. 475–476, Sept. 1976.

[14] P. Guillon and Y. Garault, "Accurate resonant frequencies of dielectric resonators," *IEEE Trans. Microwave Theory Tech.*, vol. MTT-25, pp. 916–922, Nov. 1977.

[15] E. A. J. Marcatili, "Bends in optical dielectric guides," *Bell Syst. Tech. J.*, vol. 48, pp. 2103–2132, Sept. 1969.

[16] V. Ramaswamy, "Strip-loaded film waveguide," *Bell Syst. Tech. J.*, vol. 53, pp. 697–704, Apr. 1974.

[17] E. A. J. Marcatili, "Dielectric rectangular waveguide and directional coupler for integrated optics," *Bell Syst. Tech. J.*, vol. 48, pp. 2079–2102, Sept. 1969.

[18] R. F. Harrington, *Time Harmonic Electromagnetic Fields*. New York: McGraw-Hill, 1961, ch. 5.

[19] K. Yasuura, K. Shimohara, and T. Miyamoto, "Numerical analysis of a thin-film waveguide by mode-matching method," *J. Opt. Soc. Amer.*, vol. 70, pp. 183–191, Feb. 1980.

[20] H. Aoki, "A study of dielectric pillbox resonators of an open structure," M.S. dissertation, Doshisha University, Kyoto, Japan, 1982.

[21] M. Tsuji, S. Suhara, H. Shigesawa, and K. Takiyama, "Submillimeter guided-wave experiments with dielectric rib waveguides," *IEEE Trans. Microwave Theory Tech.*, vol. MTT-29, pp. 547–552, June 1981.

[22] W. Magnus, F. Oberhettinger, and R. P. Soni, *Formulas and Theorems for the Special Functions of Mathematical Physics*. New York: Springer-Verlag, 1966, p. 144.

[23] M. Tsuji, H. Shigesawa, and K. Takiyama, "Characteristics of dielectric rib waveguide analyzed by the approximated mode-matching method and its experiments in the millimeter-wave region," *Trans. IECE Japan*, vol. 63B, pp. 884–891, Sept. 1980.

**Mikio Tsuji** (S'77–M'82) was born in Kyoto, Japan, on September 10, 1953. He received the B.S. and M.S. degrees in electrical engineering from Doshisha University, Kyoto, Japan, in 1976 and 1978, respectively.

Since 1981 he has been a Research Assistant of the Faculty of Engineering at Doshisha University. His research activities have been concerned with submillimeter-wave transmission lines and devices of open structures.

Mr. Tsuji is a member of the Institute of Electronics and Communication Engineers (IECE) of Japan.

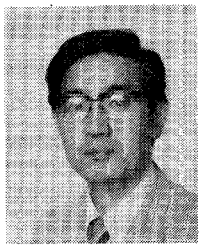

**Hiroshi Shigesawa** (S'62–M'63) was born in Hyogo, Japan, on January 5, 1939. He received the B.S., M.S., and Ph.D. degrees in electrical engineering from Doshisha University, Kyoto, Japan, in 1961, 1963, and 1969, respectively.

Since 1963 he has been with Doshisha University. From 1979 to 1980 he was a Visiting Scholar at the Microwave Research Institute, The Polytechnic Institute of New York. Currently, he is a Professor on the Faculty of Engineering. His research activities have been concerned with microwave and submillimeter-wave transmission lines and devices of open structures, fiber optics, and scattering problems of electromagnetic wave.

Dr. Shigesawa is a member of the Institute of Electronics and Communication Engineers (IECE) of Japan, the Japan Society of Applied Physics, and the Optical Society of America (OSA).

**Hitoshi Aoki** was born in Tottori, Japan, on December 3, 1954. He received the B.S. and M.S. degrees in electrical engineering from Doshisha University, Kyoto, Japan, in 1980 and 1982, respectively. He is now with Mitsubishi Electrical Corp.

Mr. Aoki is a member of the Institute of Electronics and Communication Engineers (IECE) of Japan.

**Kei Takiyama** (M'58) was born in Osaka, Japan, on October 20, 1920. He received the B.S. and Ph.D. degrees in electrical engineering from Kyoto University, Kyoto, Japan, in 1942 and 1955, respectively.

Since 1954 he has been a Professor of Electronic Engineering at Doshisha University, Kyoto, Japan, where he carried out research in the fields of microwave transmission lines and optical engineering. From 1957 to 1958 he was a Fulbright Scholar and a Research Associate at the Microwave Research Institute, the Polytechnic Institute of Brooklyn, New York.

Dr. Takiyama is a member of the Institute of Electronics and Communication Engineers (IECE) of Japan, the Institute of Electrical Engineers of Japan, and the Optical Society of America (OSA).

# Uniform Asymptotic Technique for Analyzing Wave Propagation in Inhomogeneous Slab Waveguides

HIROYOSHI IKUNO AND AKIRA YATA

*Abstract*—**The guided modes of inhomogeneous dielectric slab waveguides are analyzed by a uniform asymptotic technique based on the related equation method. This technique gives highly accurate solutions in the sense of asymptotic expansion. The algorithm for calculating the guided modes of slab waveguides with an even polynomial refractive-index medium is presented. As an example, we calculate the third-order approximate solutions for the guided modes in an analytic form. The results show that the WKB solutions for higher order modes are more accurate than for the lower order modes and the correction to the WKB solutions is significant for the lower order modes. The numerical result for eigenvalues and modal fields confirms that the third-order asymptotic solution is accurate for all the guided modes of the near-parabolic profile waveguides and for higher order modes in the case of the quasi-Gaussian profile.**

Manuscript received March 4, 1982; revised April 28, 1982.

The authors are with the Department of Information Engineering, Kumamoto University, Kumamoto 860, Japan.

## I. Introduction

RECENT ADVANCES of fabrication technology of optical integrated circuits produce optical channel waveguides and directional couplers with a great variety of inhomogeneous media including those with a Gaussian distribution. A number of design theories have been presented to evaluate the propagation characteristics of such inhomogeneous slab waveguides [1]–[4]. Although the WKB method is useful for analyzing these waveguides, it fails in the case of relatively strong inhomogeneity [4]. Considerable efforts have been made to overcome this drawback of the WKB method [5]–[9].

In this paper, we analyze the guided modes of waveguides with an even polynomial-profile medium. This pro-

0018-9480/82/1100-1958$00.75 ©1982 IEEE